

What Is Your Neurologic Diagnosis?

In collaboration with the American College of Veterinary Internal Medicine

Emma J. Suiter, BVetMed¹; Sabrina Gillespie, BVetMed²; Carlo Anselmi, DVM³; Annette Wessmann, DrMedVet^{1*}

¹Neurology-Neurosurgery Service, Pride Veterinary Centre, Derby, England

²Queen Mother Hospital for Animals, Royal Veterinary College, Brookmans Park, Hatfield, England

³Diagnostic Imaging Service, Pride Veterinary Centre, Derby, England

*Corresponding author: Dr. Wessmann (annette.wessmann@scarsdalevets.com)

<https://doi.org/10.2460/javma.21.03.0125>

Neurologic examination

Observation

Mental	Alert	X	Depressed		Disoriented		Stupor		Coma	
Posture	Normal		Tremor		Falling		Head tilt		Head turn	
Gait	Normal		Ataxia	X	Pelvic limbs	X	All 4	X	Circling	X
Paresis	Pelvic limbs		Tetra	X	Hemi		Mono			
Other	Gait assessment was limited because of the dog's lateral recumbency.									

Key: 4 = Exaggerated, clonus; 3 = Exaggerated; 2 = Normal; 1 = Diminished; 0 = None; NE = Not evaluated.

Postural reactions

	Left forelimb	Right forelimb	Left hind limb	Right hind limb
Wheelbarrow	NE	NE		
Hopping	2	2	1	1
Extensor postural thrust			NE	NE
Proprioceptive positioning	2	2	0	1
Hemistand/walk	NE	NE	NE	NE
Placing-tactile	NE	NE		
Placing-visual	NE	NE		

Spinal reflexes

	Left forelimb	Right forelimb	Left hind limb	Right hind limb
Quadriceps			2	2
Extensor carpi	2	2		
Flexion	2	2	2	2
Crossed extensor	NE	NE	NE	NE
Perineal			2	2

Cranial nerves

	L	R		L	R	Comments
II, VII-Vision menace	0	0	VIII-Nystagmus, resting	0	0	Bilateral mydriasis; bilateral xeromyocytia; suspected bilateral keratoconjunctivitis sicca; bilaterally absent dazzle and pupillary light reflexes; bilaterally reduced vestibulo-ocular reflex
II, III-Pupils resting	0	0	VIII-Nystagmus, change	0	0	
Stim L	0	0	V-Sensation	2	2	
Stim R	0	0	VII-Facial mm	2	2	
II-Fundus	2	2	V, VII-Palpebral flex	2	2	
III, IV, VI-Strabismus, resting	2	2	IX, X-Gag	2	2	
III, IV, VI, VIII-Strabismus, position	2	2	XII-Tongue	2	2	

Sensation (Locate and describe any abnormality)

Hyperesthesia	0	
Superficial pain	0	
Cutaneous reflex	2	
Deep pain	NE	

Make your assessment, then continue reading.

intermittent circling in both directions thereafter. The dog's condition deteriorated over the next day, with ambulatory paraparesis progressing to nonambulatory tetraparesis on presentation. Pain was not a presenting feature. The dog was noted to have bilateral conjunctival hyperemia, a small amount of mucopurulent discharge, and xeromycteria bilaterally. The dog had previously been healthy with no other relevant medical history.

Assessment

Anatomic diagnosis

The rule-out location for the suspected neurogenic keratoconjunctivitis sicca was the parasympathetic portion of cranial nerve VII (facial nerve) bilaterally. Rule-out locations for the blindness, mydriasis, and absent dazzle and pupillary light reflexes were both retinas, both cranial nerves II (optic nerves), the optic chiasm, and the proximal optic tract. Rule-out locations for the reduced vestibulo-ocular reflex were the vestibular system (central or peripheral components), brainstem, cranial nerve III (oculomotor nerve), cranial nerve IV (trochlear nerve), and cranial nerve VI (abducens nerve). Rule-out locations for the intermittent circling to both sides were the forebrain bilaterally and the peripheral (ie, receptors in the inner ear or cranial nerve VIII [vestibulocochlear nerve]) or central (ie, rostral portion of the medulla oblongata or cerebellum) vestibular system bilaterally. The nonambulatory tetraparesis with hind limb proprioceptive deficits was most likely a result of a focal or diffuse lesion affecting the C1-C5 spinal cord segments, brainstem, cerebellum, or cerebrum.

Likely location of a single lesion

The neurologic findings were most likely a result of multifocal brain lesions affecting the rostral and middle cranial fossa and cerebrum, cerebellum, and brainstem.

Etiologic diagnosis

The intermittent but overall progressive signs could have been a result of a single condition causing multifocal CNS lesions or, less likely, multiple condi-

tions. Differential diagnoses included recurrent cerebrovascular events (eg, an acquired coagulopathy caused by, for example, *Angiostrongylus vasorum*; immune-mediated thrombocytopenia; a concurrent medical condition such as septic or neoplastic thromboembolism; endocrine disease; intravascular lymphoma; or hypertension), meningoencephalomyelitis (infectious or immune mediated), and neoplasia (primary CNS or metastatic).

Diagnostic Plan

The diagnostic plan included a CBC and serum biochemical panel, measurement of activated partial thromboplastin and partial thromboplastin times, testing for *A vasorum* infection, measurement of blood pressure, a full ophthalmologic examination (including Schirmer tear tests), and MRI of the brain with CSF analysis.

Diagnostic Test Findings

Schirmer tear testing confirmed bilateral keratoconjunctivitis sicca with tear production of 0 mm/min in the right eye and 4 mm/min in the left eye. Intraocular examination revealed incipient equatorial cataracts and nuclear sclerosis, but the fundus appeared normal. Serum biochemical abnormalities consisted of high alkaline phosphatase (412 U/L; reference interval, 0 to 90 U/L) and aspartate aminotransferase (128 U/L; reference interval, 0 to 20 U/L) activities. Results of CBC as well as blood pressure, activated partial thromboplastin time, and partial thromboplastin time were within reference limits. Results of an ELISA for *A vasorum* antigen were negative.

Magnetic resonance imaging of the brain was performed with a 1.5-T unit (Signa HDx 1.5T MRI; GE Healthcare), with images obtained before and after contrast (gadolinium) administration. An oval, expansile, lytic mass was observed within the presphenoid bone, the rostral aspect of the basisphenoid bone, and the adjacent aspects of the pterygoid and palatine bones (**Figures 1 and 2**). There was diffuse

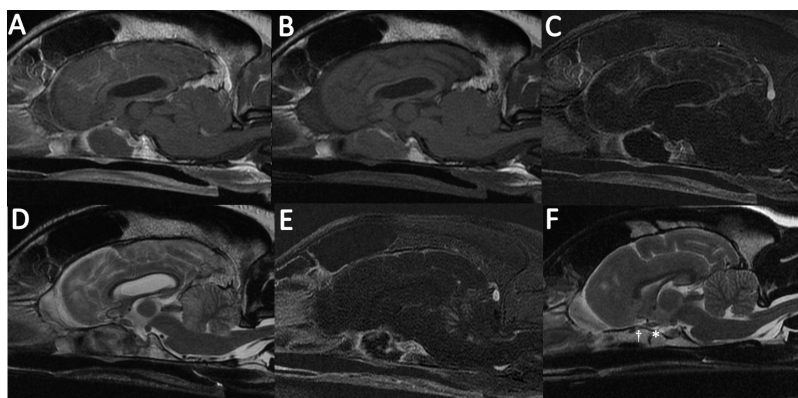


Figure 1—Sagittal and parasagittal MRI images of the brain of a 12-year-old Border Collie with acute-onset blindness, bilateral xeromycteria, neurogenic keratoconjunctivitis sicca, nonambulatory tetraparesis, and hind limb proprioceptive deficits (A through E) and a sagittal MRI image of the brain of a healthy dog for comparison (F). The sphenoid bone is isointense to the gray matter on a T1-weighted image (A) with mild heterogeneous, mainly peripheral contrast enhancement (B). On a sagittal view in subtraction, a hypointense mass expanding from the sphenoid bone can be seen (C). The mass has mixed intensity on a T2-weighted image, and the cortical margins of the sphenoid bone are indistinct, with lysis and ventral extension of abnormal tissue into the nasopharynx (D). There is a triangular hyperintensity in the rostral portion of the left cerebellum on a parasagittal saturation image (E). In the healthy dog (F), notice the normal presphenoid bone (asterisk) and basisphenoid bone (dagger).

of the sphenoid bone are indistinct, with lysis and ventral extension of abnormal tissue into the nasopharynx (D). There is a triangular hyperintensity in the rostral portion of the left cerebellum on a parasagittal saturation image (E). In the healthy dog (F), notice the normal presphenoid bone (asterisk) and basisphenoid bone (dagger).

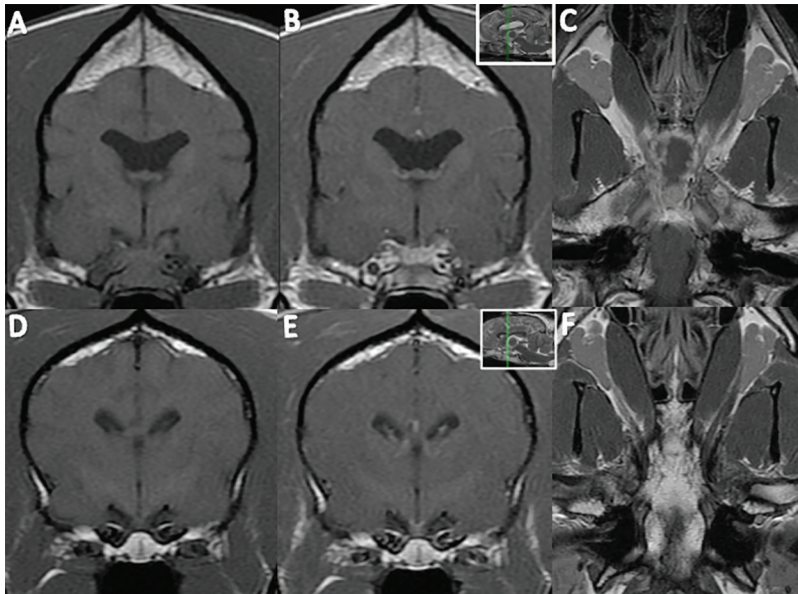


Figure 2—Transverse and dorsal MRI images of the brain of the Border Collie in Figure 1 (A through C) and similar transverse and dorsal MRI images of the brain of a healthy dog of similar age and skull conformation for comparison (D through F). The transverse images were obtained at the most probable and perceived level of the pterygoid canal (inset; dotted line). The expansile lytic mass involving the sphenoid mass was isointense to the gray matter in a T1-weighted image (A) and had diffuse, mild contrast enhancement (B). A dorsal view of the sphenoid bone shows marked contrast uptake with loss of the normal bone marrow fat signal and a central lack of contrast enhancement on a postcontrast T1-weighted image (C). The normal appearance (note the normal bone marrow fat signal of the sphenoid bone) is evident in T1-weighted precontrast (D) and postcontrast (E and F) images of the healthy dog.

effacement of the expected bone marrow fat signal of these bones. The lesion was heterogeneously hyperintense on T2-weighted and STIR images and hypointense on T1-weighted images with mild heterogeneous patchy contrast enhancement. Cortical margins of the sphenoid bone were indistinct, with a periosteal reaction, evidence of lysis, and abnormal soft tissue extending into the nasopharynx. The adjacent pachymeninges showed marked contrast enhancement. In the rostral aspect of the left cerebellum, there was a large, well-defined, triangular intra-axial lesion that was hyperintense on T2-weighted and STIR images and isointense on T1-weighted images with mild, patchy contrast enhancement. This lesion demonstrated no mass effect. Additional smaller, well-defined, intra-axial lesions were noted in the rostral aspect of the right cerebellum and the periventricular white matter. Similarly, these lesions were hyperintense on T2-weighted and STIR images and isointense on T1-weighted images with mild patchy contrast enhancement. The MRI findings of the sphenoid bone were compatible with osteomyelitis or neoplasia (eg, osteosarcoma, chondrosarcoma, or lymphoma). The lesions within the rostral cerebellum and periventricular region were most consistent with ischemic infarctions. Analysis of a cisternal CSF sample revealed a slightly high total nucleated cell count (18 cells/ μ L; reference interval, < 5 cells/ μ L) consisting of 55% neutrophils, 30% monocytes, and occasional reactive lymphocytes. The CSF total protein concentration was 47 mg/dL (reference interval, < 25 mg/dL).

Results of thoracic CT, performed with a commercial unit (Brightspeed 16 CT; GE Healthcare), were unremarkable. On abdominal ultrasonography, the liver was heterogeneous and irregularly marginated. Multiple, round, well-defined hyperechoic nodules (all < 1 cm in diameter) were detected in the spleen. Results of cytologic examination of fine-needle aspirates of the sphenoid bone obtained via the soft palate were nondiagnostic. Cytologic examina-

tion of fine-needle aspirates of the liver demonstrated a moderate degree of hepatocyte cytoplasmic rarefaction but no neoplastic cells. Cytologic examination of fine-needle aspirates of the spleen revealed an atypical round cell population that had multiple criteria for malignancy. A PCR assay for antigen receptor rearrangement indicated the presence of clonal B-lymphocytes, which was 95% specific for a diagnosis of lymphoma or leukemia.

Overall, the diagnostic findings were most consistent with lymphoma of the sphenoid bones and spleen.

Treatment

Owing to financial constraints and the guarded prognosis, palliative care was initiated. The patient was treated with prednisolone (2 mg/kg, PO, q 24 h) at an immunosuppressive dosage. The neurogenic keratoconjunctivitis sicca was treated with artificial tears and 2% pilocarpine drops to increase tear production. Although an initial improvement was seen, euthanasia was elected approximately 6 weeks later because of lethargy, vomiting, and a reluctance to move. At necropsy, histologic examination of the sphenoid bones and surrounding tissues revealed a malignant round cell neoplasm compatible with lymphoma or chronic lymphocytic leukemia with histologic evidence of metastatic spread to the spleen, liver, and kidney.

Comments

Reports of skull-based tumors are rare in the veterinary and human literature, and, to our knowledge, the present report represented the first report of lymphoma affecting the sphenoid bones in a dog and causing blindness and neurogenic keratoconjunctivitis sicca. Only 2 case reports have described a similar presentation, with disease of the sphenoid bones caused by a disseminated mast cell tumor in a

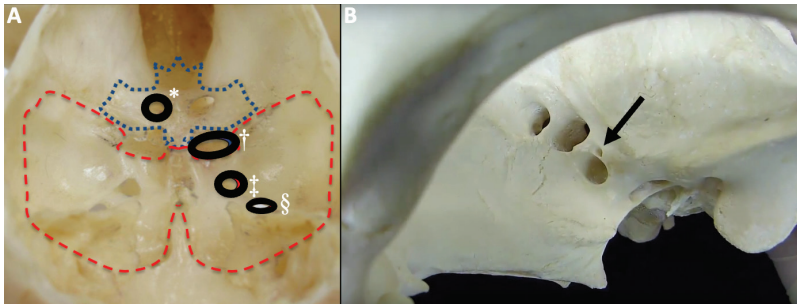


Figure 3—Photographs of the skull of a clinically normal dog. A—On a dorsal view following removal of the calvarium, the optic canal (asterisk), orbital fissure (dagger), round foramen (double dagger), and oval foramen (silcrow) can be seen. The presphenoid (blue dotted line) and basisphenoid (red dashed line) bones are indicated. B—On a lateral view of the skull, the pterygoid canal (arrow) can be seen. Images provided by Drs. Elsa Beltran (A) and Sabrina Gillespie (B).

dog in one report¹ and by osteomyelitis in 2 dogs and a cat in the other report.² Reported clinical signs included decreased to absent visual and pupillary light reflexes and vestibulo-ocular reflexes.^{1,2} The dog described in the present report also had dysfunction of the parasympathetic portion of the facial nerve characterized by neurogenic keratoconjunctivitis sicca. In humans, primary skull-based lymphoma has been described with concurrent cranial nerve VII deficits.³ However, other reported signs such as diplopia (double vision), trigeminal hyperesthesia, headache, fevers, night sweats, weight loss, and hearing loss³ were not reported in our dog.

In our dog, the multiple cranial nerve dysfunction was caused by an expansile tumor affecting the sphenoid bones and adjacent structures leading to blindness (cranial nerve II), mydriasis (cranial nerves II and III), and a reduced vestibulo-ocular reflex (cranial nerves III, IV, and VI). Anatomically, the afferent pathway of cranial nerve II travels through the optic canal of the presphenoid bone, and the efferent pathways of cranial nerves III, IV, and VI exit through the orbital fissure, located between the basisphenoid and presphenoid bones.⁴ Cranial nerve VII leaves the brainstem together with cranial nerve VIII, entering the facial canal in the petrous temporal bone. Here, cranial nerve VII divides into motor and parasympathetic branches. The motor branch emerges at the stylomastoid foramen located dorsolateral to the tympanic bulla and distributes to the muscles of facial expression and the caudal portion of the digastric muscle. This branch was unaffected in our dog, resulting in a normal facial expression. The parasympathetic branch of cranial nerve VII gives rise to the major petrosal and chorda tympani nerves. The major petrosal nerve extends through the pterygoid bone in the pterygoid canal, exiting near the round foramen to synapse in the pterygopalatine ganglion and from there innervates the lacrimal glands and nasal mucosa (**Figure 3**).⁴ Bilateral involvement of the pterygoid canal by the expansile lesion in the dog described in the present report likely caused parasympathetic dysfunction of the major petrosal nerves bilaterally, resulting in bilateral neurogenic keratoconjunctivitis sicca.

The intermittent circling to both sides and recumbency in this dog can be explained by vascular infarcts of the rostral cerebellum and periventricular region.⁵ The cerebellum is a common site for ischemic stroke.⁵ The infarcts in this dog were presumed to be secondary to neoplastic emboli; how-

ever, septic emboli or thrombi were also possible. A retrospective study⁶ investigating concurrent medical conditions in 18 dogs with brain infarcts found that only 2 had neoplasia. However, not all dogs in that study underwent complete imaging or medical investigations, and concurrent neoplasia may have been underdiagnosed.

When presented with an animal with blindness, mydriasis, and reduced vestibulo-ocular reflexes, practitioners should remember that the common anatomic exit points of the associated nerves may indicate a lesion affecting the base of the skull, with neoplasia as an important differential diagnosis. Furthermore, purely parasympathetic dysfunction of the facial nerve can occur with extensive skull-based tumors, presenting as neurogenic keratoconjunctivitis sicca with a normal facial expression.

Acknowledgments

The authors thank Dr. Ian David Jones for help with the initial imaging report and Dr. Elsa Beltran for providing image (A) of Figure 3.

References

1. Beltran E, de Stefani A, Stewart J, De Risio L, Johnson V. Disseminated mast cell tumor infiltrating the sphenoid bone causing blindness in a dog. *Vet Ophthalmol*. 2010;13(3):184-189. doi:10.1111/j.1463-5224.2010.00776.x
2. Busse C, Dennis R, Platt SR. Suspected sphenoid bone osteomyelitis causing visual impairment in two dogs and one cat. *Vet Ophthalmol*. 2009;12(2):71-77. doi:10.1111/j.1463-5224.2008.00678.x
3. Marinelli JP, Modzeski MC, Lane JL, et al. Primary skull base lymphoma: manifestation and clinical outcomes of a great imitator. *Otolaryngol Head Neck Surg*. 2018;159(4):643-649. doi:10.1177/0194599818773994
4. De Lahunta A. Lower motor neuron: general somatic efference, cranial nerve. In: De Lahunta A, Glass E, Kent M, eds. *Veterinary Neuroanatomy and Clinical Neurology*. 4th ed. Elsevier Saunders; 2015:162-196.
5. Garosi L, McConnell JF, Platt SR, et al. Clinical and topographic magnetic resonance characteristics of suspected brain infarction in 40 dogs. *J Vet Intern Med*. 2006;20(2):311-321. doi:10.1892/0891-6640(2006)20[311:catmrc]2.0.co;2
6. Garosi L, McConnell JF, Platt SR, et al. Results of diagnostic investigations and long-term outcome of 33 dogs with brain infarction (2000-2004). *J Vet Intern Med*. 2005;19(5):725-731. doi:10.1892/0891-6640(2005)19[725:rodial]2.0.co;2